Optics Communications 281 (2008) 5889–5893

Contents lists available at ScienceDirect

Optics Communications

journal homepage: www.elsevier.com/locate/optcom

Femtosecond pulse propagation in silicon waveguides: Variational approach and its advantages

Samudra Roy [a], Shyamal K. Bhadra [a,*], Govind P. Agrawal [b]

[a] Fiber Optics Laboratory, Central Glass and Ceramic Research Institute, CSIR, 196 Raja S.C. Mullick Road, Kolkata-700 032, West Bengal, India
[b] Institute of Optics, University of Rochester, Rochester, NY 14627, USA

ARTICLE INFO

Article history:
Received 5 August 2008
Received in revised form 19 August 2008
Accepted 19 August 2008

ABSTRACT

We investigate the propagation characteristics of ultrafast pulses inside silicon waveguides considering frequency chirp associated with each input pulse. Effects of linear losses, two-photon absorption, and free-carrier dynamics are included analytically within the framework of a modified variational formalism and the results are validated by comparing them with full numerical simulations. It is found that an initial chirp helps in maintaining the pulse shape and spectrum in the anomalous-dispersion regime, thereby resulting in soliton-like propagation of ultrashort optical pulses.

1. Introduction

Silicon photonics has attracted a great deal of attention in the recent years because of its broad application domain covering optoelectronic integration to biosensing [1,2]. Silicon has excellent linear and nonlinear properties in the mid-infrared spectral region that are useful for variety of applications related to emerging photonics devices. The optical mode inside a silicon-on-insulator (SOI) waveguides is tightly confined to a rib-like structure because of the high refractive index of silicon (~3.45) compared to the air or silica acting as a clad. The high values of the Kerr coefficient (nearly 100 times larger than that of silica glass) and Raman gain coefficient (nearly 1000 times larger than that of silica glass) lead to efficient nonlinear interaction with optical fields at relatively low power levels [3,4]. For this reason, SOI waveguides have been used to produce broadband amplifier and tunable lasers exploiting the nonlinear effects such as Raman amplification [5–7] and four-wave mixing [8]. They have also been used for spectral broadening of ultrashort optical pulses through self phase modulation [9] and supercontinuum generation [10]. The possibility of forming a stable optical soliton inside a SOI waveguide is also being investigated because the pulse width can then be maintained close to its input value [11,12]. Experimentally, it is observed that solitons can be formed inside a 5 mm long SOI waveguide by launching femtosecond pulses with sub-picojoule energy [12]. However, the linear loss, two-photon absorption (TPA), and free-carrier absorption (FCA) influence the pulse shape and spectrum significantly [11]. Indeed, these loss mechanisms are considered to be a major obstacle for soliton formation in SOI waveguides.

The modeling of pulse propagation inside SOI waveguides requires numerical solution of a generalized nonlinear Schrödinger equation. Although a numerical scheme is eventually necessary for validating the experimental data, its exclusive use often limits physical insight into the nonlinear processes that govern the propagation process. In the present paper, we exploit the variational formalism for studying the parametric effects on a femtosecond pulse inside a SOI waveguide. The main limitation of the variational technique is that it requires the functional form of the pulse shape to remain the same even though the parameters of the pulse such as its amplitude, width, phase, and chirp are allowed to change during propagation. In the case of soliton-like propagation, the pulse dynamics can well be treated with the help of a variational process since the pulse shape is expected to remain close to that of the input pulse during propagation. An advantage of this method is that, the perturbing effects of linear loss, TPA, and FCA can be treated by introducing Rayleigh's dissipation function (RDF) [13–15]. Such a semi-analytical approach leads to a set of ordinary differential equations for the pulse parameters such as amplitude, width, phase, and chirp. We stress that the time-dependent free-carrier dynamics is included in our derivation to the variational equations. These equations not only provide considerable physical insight, they can also be solved rapidly over a large range of the parameter space. We find the regime of validity of the variational technique by comparing its predictions with the numerical solution obtained by solving the generalized nonlinear Schrödinger equation with the standard split-step algorithm [16].

2. Theoretical model

The propagation of an optical pulse through a SOI waveguide is governed by the extended nonlinear Schrödinger equation [11] given by

* Corresponding author.
E-mail address: skbhadra@cgcri.res.in (S.K. Bhadra).

0030-4018/$ - see front matter © 2008 Elsevier B.V. All rights reserved.
doi:10.1016/j.optcom.2008.08.030

$$\frac{\partial u}{\partial z}+\frac{i\beta_2}{2}\frac{\partial^2 u}{\partial t^2}-\frac{\beta_3}{6}\frac{\partial^3 u}{\partial t^3}=i\gamma\mid u\mid^2 u-\Gamma\mid u\mid^2 u-\frac{\alpha_l}{2}u-\frac{\sigma}{2}N_C u, \tag{1}$$

where u, β_2, β_3, γ, Γ, α_l, σ, and N_C represent the slowly varying field amplitude, second-order dispersion coefficient, third-order dispersion coefficient, nonlinear Kerr coefficient, TPA coefficient, linear loss parameter, FCA coefficient, and free carrier density, respectively. Since the TPA-induced free-carrier density N_C has a profound effect on the pulse amplitude, the dynamic nature of N_C is included by solving the rate equation [3],

$$\frac{dN_C}{dt}=\frac{\beta_{TPA}}{2h\nu_0 a_{eff}^2}\mid u(z,t)\mid^4-\frac{N_C}{\tau_C}, \tag{2}$$

where τ_C is the carrier life time, $h\nu_0$ is the photon energy at the incident wavelength, a_{eff} is the effective mode area, and $\beta_{TPA}=2\Gamma a_{eff}$ is the usual TPA parameter.

For a short optical pulse ($t_0 \ll \tau_C$), one can ignore τ_C, as carriers do not have enough time to recombine over the pulse duration. In this situation, it is possible to solve Eq. (2) analytically for a given optical field. We assume that the sech-type shape of the input pulse remains unchanged during propagation but allows its parameter to evolve with the propagation distance z. In this case, a suitable form of the optical field is

$$u(z,t)=A\,\mathrm{sech}\left(\frac{t}{t_0}\right)\exp\left[i\left\{\phi-\frac{C}{2}\frac{t^2}{t_0^2}\right\}\right], \tag{3}$$

where A, t_0, φ, and C represent the amplitude, width, phase, and chirp, respectively, and all of them vary with z. For this pulse shape, we can solve Eq. (2) analytically, and the carrier density is found to be

$$N_C=\frac{\beta_{TPA}A^4 t_0}{2h\nu_0 a_{eff}^2}\left[\frac{2}{3}+\left\{\tanh\left(\frac{t}{t_0}\right)-\frac{1}{3}\tanh^3\left(\frac{t}{t_0}\right)\right\}\right]. \tag{4}$$

To solve Eq. (1) with the variational technique, we first find the Lagrangian and the RDF associated with it. They are given by

$$L=\frac{1}{2}(uu_z^*-u^*u_z)+\frac{i\beta_2}{2!}\mid u_t\mid^2-\frac{1}{2}\frac{\beta_3}{3!}(u_t^*u_{tt}-u_tu_{tt}^*)+\frac{i\gamma}{2}\mid u\mid^4 \quad \text{and} \tag{5}$$

$$R=\Gamma(uu_z^*-u^*u_z)\mid u\mid^2+\frac{\alpha}{2}(uu_z^*-u^*u_z)+\frac{1}{2}\sigma N_C(uu_z^*-u^*u_z). \tag{6}$$

The reduced form of Lagrangian and RDF is obtained by integrating them over time [14]:

$$L_g=\int_{-\infty}^{\infty}L\,dt \qquad R_g=\int_{-\infty}^{\infty}R\,dt. \tag{7}$$

With the help of Eqs. (3)–(7), we obtain the following explicit expressions of L_g and R_g:

$$L_g=-iA^2\left[2t_0\frac{\partial\phi}{\partial z}-\frac{\pi^2}{6}\left\{\frac{t_0}{2}\frac{\partial C}{\partial z}-C\frac{\partial t_0}{\partial z}\right\}\right]+i\frac{\beta_2A^2}{3t_0}\left[1+\frac{C^2\pi^2}{4}\right]+i\frac{2}{3}\gamma A^4t_0 \tag{8}$$

$$R_g=(-2i)\frac{\partial\phi}{\partial z}\left[\frac{4}{3}\Gamma A^4t_0+\alpha t_0A^2+\frac{2}{3}\sigma\left(\frac{\beta_{TPA}A^6t_0^2}{2h\nu_0a_{eff}^2}\right)\right]+2i\left[\frac{t_0}{2}\frac{\partial C}{\partial z}-C\frac{\partial t_0}{\partial z}\right]\left[\frac{(\pi^2-6)}{9}\Gamma A^4+\frac{\pi^2}{12}\alpha A^2+\frac{\pi^2}{18}\sigma\left(\frac{\beta_{TPA}A^6t_0}{2h\nu_0a_{eff}^2}\right)\right] \tag{9}$$

The final step is to employ the Euler–Lagrange equation in the form

$$\frac{d}{dt}\left(\frac{\partial L_g}{\partial q_z}\right)-\frac{\partial L_g}{\partial q}+\frac{\partial R_g}{\partial q_z}=0, \tag{10}$$

where $q = A$, t_0, φ or C and the suffix z indicates the corresponding derivatives. For each q, we obtain an ordinary differential equation, resulting in the following set of four coupled equations:

$$\frac{\partial A}{\partial z}=-\frac{\alpha_l}{2}A-\left(\frac{\beta_2C}{2t_0^2}\right)A-2\Gamma\left(\frac{1}{\pi^2}+\frac{1}{3}\right)A^3-\frac{\sigma}{3}\left(\frac{\Gamma A^5t_0}{h\nu_0a_{eff}}\right) \tag{11}$$

$$\frac{\partial t_0}{\partial z}=\frac{\beta_2C}{t_0}+\frac{4}{\pi^2}\Gamma A^2t_0 \tag{12}$$

$$\frac{\partial C}{\partial z}=\frac{8}{\pi^2}\Gamma A^2C+\frac{\beta_2}{t_0^2}\left(\frac{4}{\pi^2}+C^2\right)+\frac{4}{\pi^2}\gamma A^2 \tag{13}$$

$$\frac{\partial\phi}{\partial z}=\frac{\beta_2}{3t_0^2}+\frac{5}{6}\gamma A^2. \tag{14}$$

The variational Eqs. (11)–(14) show clearly how the pulse parameters change during the propagation inside a SOI waveguide and how they are coupled with each other. More to the point, they show which linear and nonlinear process affect a particular pulse parameter. Considerable physical insight is gained by noting that the pulse width in Eq. (12) is affected directly not only by the dispersion parameter (as expected) but also by the TPA (somewhat unexpected). Moreover, whereas dispersion may lead to pulse broadening or compression depending on the sign of β_2, TPA always leads to the pulse broadening. It may be noted that β_3 does not appear in Eqs. (11)–(14). It is well known [16] thatβ_3 introduces a relatively small temporal shift of the pulse center that we ignore here. Also, if the carrier frequency of the pulse shifts, it changes the effective value of β_2. Since no such frequency shift occurs in our case, β_3 does not affect the major pulse parameters.

Eq. (12) shows that waveguide dispersion can introduce pulse compression when the pulse is suitably chirped. More specifically, pulse compression occurs if the condition $\beta_2C<0$ is maintained throughout the propagation distance. Similarly, as expected, the pulse amplitude in Eq. (11) is affected by the three loss mechanisms (linear loss, TPA, and FCA). However, somewhat surprisingly, it is also affected by dispersion when pulse is chirped. The chirp itself is affected by the Kerr nonlinearity, waveguide dispersion, and by the TPA process. In the next section we discuss the effect of input chirping on pulse evolution and show that an initial chirp of the pulse can help in propagating it as a soliton. We ignore the phase equation in the following discussion because the optical phase does not affect the three most relevant pulse parameters (A, t_0, and C).

3. Results and discussion

To investigate the possibility of soliton formation, we begin by focusing on femtosecond pulses propagating in the anomalous-dispersion region of a silicon waveguide. Table 1 shows the values of device and pulse parameters employed in our study. We solve the set of three coupled equations, Eqs. (11)–(13), using Matlab software and compare in Fig. 1a the results for input pulses that are either initially unchirped (dashed lines) or chirped suitably (solid

Table 1
Values of the parameters used for numerical calculation

Parameter name	Symbol	Value
Waveguide length	L	1 cm
Linear loss	α_l	22 dB/m
Effective area	a_{eff}	0.38 μm^2
Group velocity dispersion	β_2	±0.56 ps^2/m
Nonlinear coefficient	γ	47 m^{-1} W^{-1}
Nonlinear loss	Γ	6.5 m^{-1} W^{-1}
Wavelength	λ_0	1550 nm
Input peak power	P_0	4.76 Watt
Pulse width	$t_0(0)$	50 fs

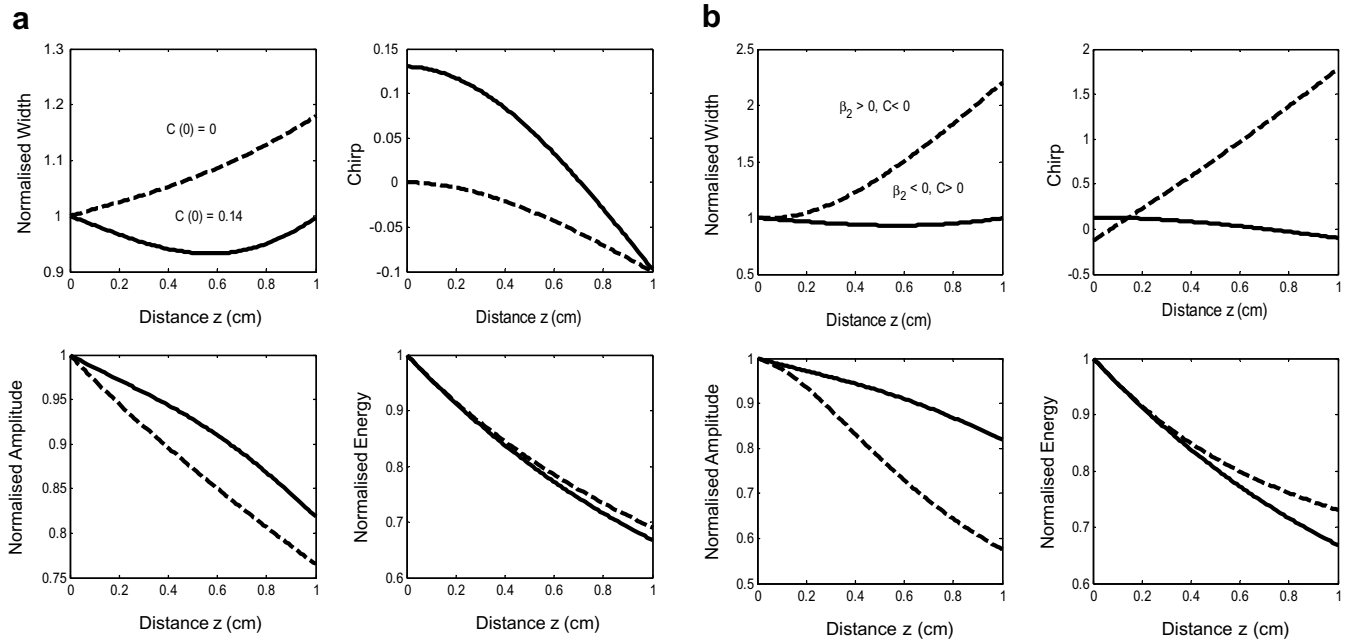

Fig. 1. (a) Evolution of pulse, width, chirp, amplitude, and energy for initially chirped (solid line) and unchirped (dashed line) pulses. (b) Effect of normal (dashed lines) and anomalous (solid lines) dispersion on pulse parameters. Input pulses are chirped in both cases such that $\beta_2 C < 0$. The used chirp values are 0.14 (solid lines) and −0.14 (dashed lines), respectively.

lines) to ensure that its width nearly remains unchanged at the output end. The important point to note is that the pulse width increases monotonically for unchirped pulses because of the amplitude decay resulting from linear and nonlinear losses. In contrast, when the input pulse is slightly chirped ($C = 0.14$), the width first decreases before increasing such that the output pulse width is nearly equal to its input value. These results suggest that soliton-like propagation in a SOI waveguide can be realized in spite of losses by optimizing the input chirp.

We compare in Fig. 1b the parametric evolution of a chirped pulse in the normal and anomalous dispersion regions. In both cases, the pulse is suitably chirped so that the condition $\beta_2 C < 0$ is valid at $z = 0$. Since $\beta_2 C < 0$ initially, the pulse begins to compress, as evident from the width plot. However, this condition is violated soon after for pulses propagating in the normal-dispersion regime and their width begins to increase rapidly. In contrast, pulse continues to compress until z exceeds 5 mm in the case of anomalous dispersion. As a result, the pulse width is nearly the same as that of the input pulse when it exits the waveguide. This difference is a consequence of the fact that the SPM-induced chirp adds to the dispersion-induced chirp in the case of normal dispersion but subtracts when dispersion is anomalous [16] and is behind of soliton formation in the latter case. This conclusion is also supported by Fig. 2 where we compare the temporal and spectral profiles of the input (dotted curves) and output (solid curves) pulses in the regime of anomalous dispersion. As seen there, in the case of chirped input pulses, both the pulse shapes and spectra almost coincide. In contrast, when input pulses are unchirped, the output pulse (dashed curve) broadens considerably because of linear and nonlinear losses.

We next investigate how trustworthy is the variational approach used in obtaining the results shown in Figs. 1 and 2. For this purpose, we solve the original nonlinear Schrödinger equation given in Eq. (1) with the split-step Fourier method [16] and compare

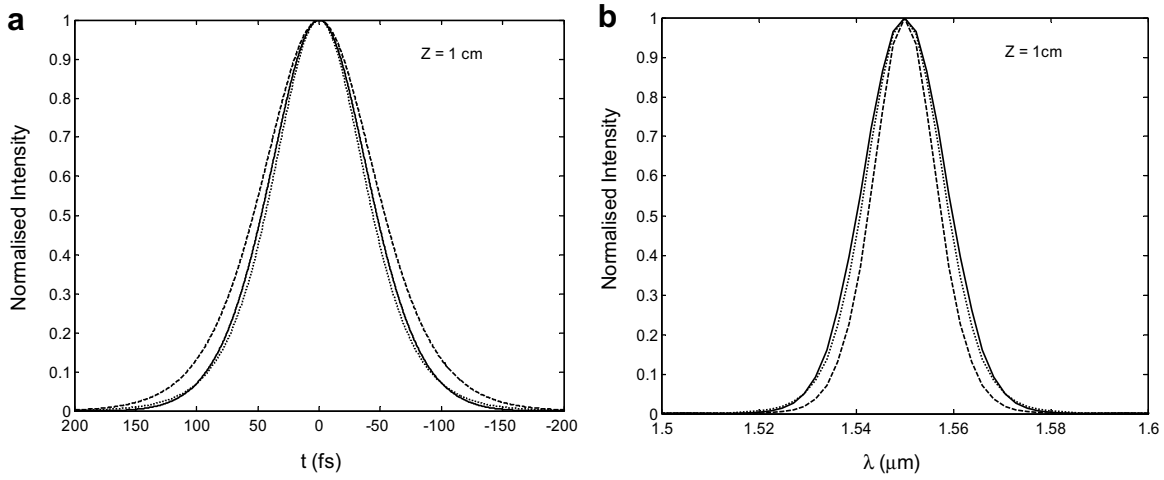

Fig. 2. Comparison of input (dotted curve) and output pulse shape (a) and spectrum (b) for initially chirped (solid line) and unchirped (dashed line) pulse.

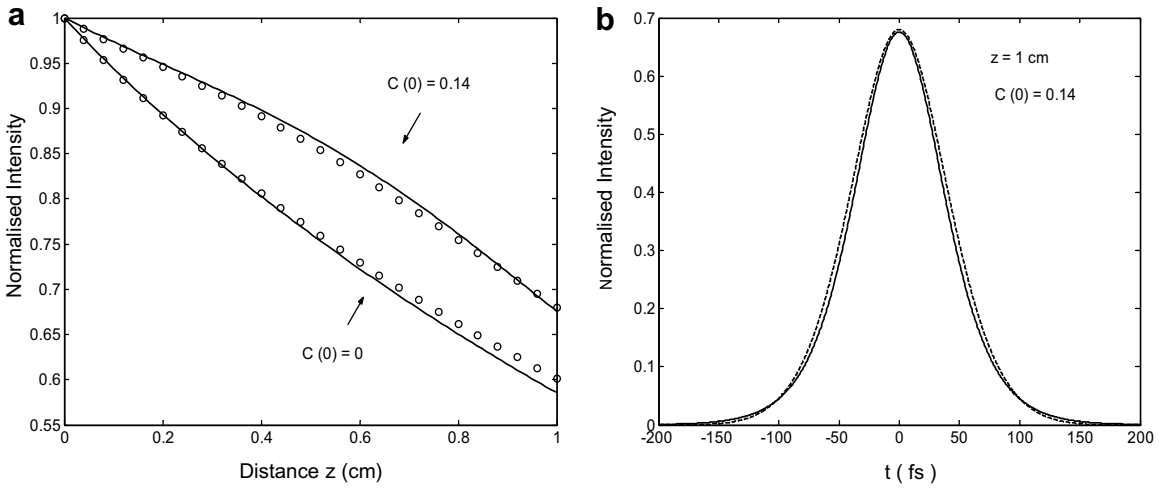

Fig. 3. (a) Evolution of the normalized amplitude for input pulses with and without an initial chirp. The solid lines represent the variational solution whereas the open circles are the corresponding numerical data. (b) Comparison of the output pulse shape; the dashed and solid curves represent the numerical and variational solutions, respectively.

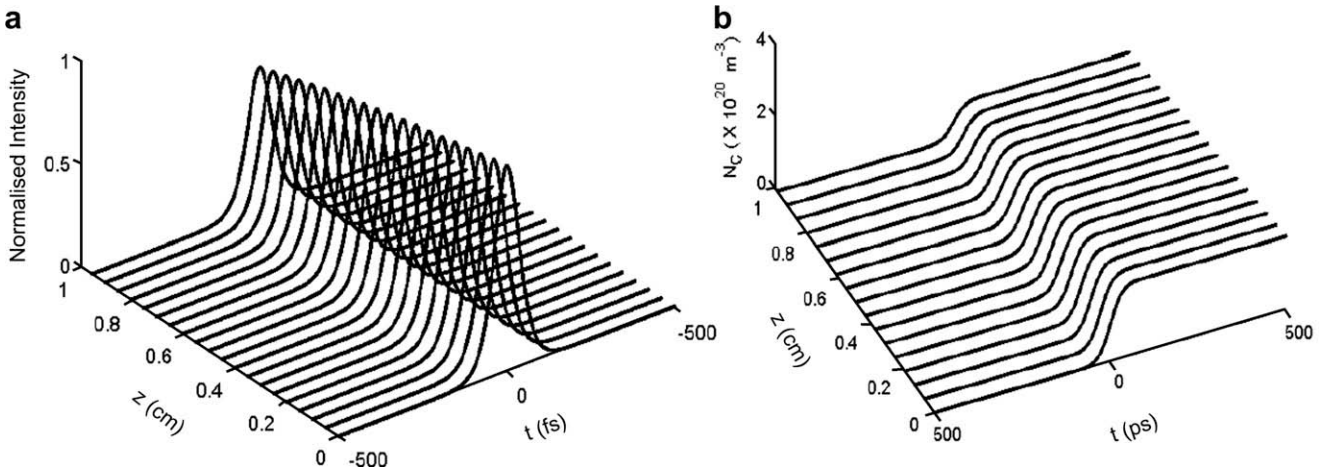

Fig. 4. (a) Soliton-like propagation nature of an initially chirped pulse and (b) the dynamic evolution of the free carrier density over the propagation distance.

the results with those obtained using the variation Eqs. (11)–(13). Fig. 3 shows the comparison in the case of anomalous dispersion for both the chirped and unchirped input pulses. The peak intensity of the pulse displayed in Fig. 3a shows that the pulse amplitude in all cases is reduced considerably because of linear loss and nonlinear losses resulting from TPA and FCA. The important point to note is that the variational results agree with the numerical data to within a few percent. The predicted output pulse in the two cases is compared in Fig. 3b. Again, the numerical output (dashed curve) agrees well with the variational prediction (solid curve).

As mentioned earlier, we were able to include the temporal variations of the TPA-generated carrier density N_C through the analytic expression given in Eq. (4). Of course, N_C also varies with z because it depends on the local value of the pulse intensity. Fig. 4 shows the soliton-like propagation of a chirped pulse together with the corresponding changes in the carrier density. As expected, the carrier density builds up continuously over the pulse duration and acquires its maximum value nearing the trailing edge of the pulse. The maximum value of carrier density does not remain constant along the waveguide length but decays gradually with increasing distance. As is evident from Eq. (4), the generation of carrier density is mainly governed by the intensity of the propagating pulse which itself decays with distance owing to linear and nonlinear losses. However, the pulse maintains its shape and width in spite of its reduced peak amplitude because of chirp-induced pulse compression.

In conclusion, the propagation dynamics of ultrashort optical pulses inside a silicon waveguide can be described reasonably well in the soliton regime with a modified variational technique. The resulting set of dynamic equations can be solved relatively easily to study the evolution of important pulse parameters such as the width, chirp, and peak intensity. Our procedure is capable of including the carrier density dynamics quite accurately. We have shown that the input chirp plays an impotent role in maintaining the pulse shape and spectrum and is useful for realizing soliton-like propagation of optical pulses. We have employed the split-step Fourier method to solve the extended nonlinear Schrödinger equation directly and to verify the accuracy of the variational results.

Acknowledgements

Authors wish to thank Dr. H. S. Maiti, Director, CGCRI, for his continuous encouragement, guidance, and support in this work. They also wish to thank the staff members of the Fiber Optic Laboratory at CGCRI for their unstinted cooperation and help.

One of the authors (S.R.) is indebted to Council of Scientific and Industrial Research (CSIR) for financial support in carrying out this work.

References

[1] B. Jalali, S. Fathpour, IEEE J. Lightwave Technol. 24 (2006) 4600.
[2] R. Soref, IEEE J. Sel. Top. Quantum Electron. 12 (2006) 678.
[3] L. Yin, G.P. Agrawal, Opt. Lett. 32 (2007) 2031.
[4] Q. Lin, O.J. Painter, G.P. Agrawal, Opt. Express 15 (2007) 16604.
[5] R. Claps, D. Dimitropoulos, V. Raghunathan, Y. Han, B. Jalali, Opt. Express 11 (2003) 1731.
[6] H. Rong, A. Liu, R. Jones, O. Cohen, D. Hak, R. Nicolaescu, A.W. Fang, M.J. Paniccia, Nature 433 (2005) 292.
[7] H. Rong, R. Jones, A. Liu, O. Cohen, D. Hak, A.W. Fang, M.J. Paniccia, Nature 433 (2005) 725.
[8] H. Fukuda, K. Yamada, T. Shoji, M. Takahashi, T. Tsuchizawa, T. Watanabe, J. Takahashi, S. Itabashi, Opt. Express 13 (2005) 4629.
[9] H.K. Tsang, C.S. Wong, T.K. Liang, Appl. Phys. Lett. 80 (2002) 416.
[10] L. Yin, Q. Lin, G.P. Agrawal, Opt. Lett. 32 (2007) 391.
[11] L. Yin, Q. Lin, G.P. Agrawal, Opt. Lett. 31 (2006) 1295.
[12] J. Zhang, Q. Lin, G. Piredda, R.W. Boyd, G.P. Agrawal, P.M. Fauchet, Opt. Express 15 (2007) 7682.
[13] H. Goldstein, Classical Mechanics, second ed., Narosa Publishing House, 2001, p. 24.
[14] D. Anderson, Phys. Rev. A 27 (1983) 3135.
[15] S. Roy, S.K. Bhadra, Physica D – Nonlinear Phenomena 232 (2) (2007) 103.
[16] G.P. Agrawal, Nonlinear Fiber Optics, fourth ed., Academic Press, Boston, 2007.